

**REGIONAL BODY-WAVE CORRECTIONS AND SURFACE-WAVE TOMOGRAPHY MODELS
TO IMPROVE DISCRIMINATION**

William R. Walter, Michael E. Pasyanos, Arthur J. Rodgers, Kevin M. Mayeda, and Alan Sicherman

Lawrence Livermore National Laboratory

Sponsored by National Nuclear Security Administration
Office of Nonproliferation Research and Engineering
Office of Defense Nuclear Nonproliferation

Contract No. W-7405-ENG-48

ABSTRACT

Our identification research for the past several years has focused on the problem of correctly discriminating small-magnitude explosions from a background of earthquakes, mining tremors, and other events. Small magnitudes lead to an emphasis on regional waveforms. The goal is to reduce the variance within the population of each type of event, while increasing the separation between the explosions and the other event types. We address this problem for both broad categories of seismic waves, body waves, and surface waves. First, we map out the effects of propagation and source size in advance so that they can be accounted for and removed from observed events. This can dramatically reduce the population variance. Second, we try to optimize the measurement process to improve the separation between population types.

For body waves we focus on the identification power of the short-period regional phases Pn, Pg, Sn and Lg, and coda that can often be detected down to very small magnitudes. It is now well established that particular ratios of these phases, such as 6- to 8-Hz Pn/Lg, can effectively discriminate between closely located explosions and earthquakes. To extend this discrimination power over broad areas, we developed a revised Magnitude and Distance Amplitude Correction (MDAC2) procedure (Walter and Taylor, 2002). This joint source and path model fits the observed spectra and removes magnitude and distance trends from the data. It allows for the possibility of variable apparent stress scaling in earthquakes, an unresolved issue that is the subject of investigation under separate funding. The MDAC2 procedure makes use of the extremely stable coda estimates of Mw for source magnitude and can also use independent Q tomography to help reduce trade-offs in fitting spectra. We can then apply the kriging operation to the MDAC2 residuals to provide full 2-D path corrections by phase and frequency band. These corrections allow the exploration of all possible ratios and multivariate combinations of ratios for their discrimination power. We also make use of the MDAC2 spectra and the noise spectra to determine the expected signal-to-noise value of each phase and use that to optimize the multivariate discriminants as a function of location. We quantify the discrimination power using the misidentified event trade-off curves and an equi-probable measure. In addition to the traditional phases, we are also exploring the application of coda amplitudes in discrimination. Coda-derived spectra can be peaked due to Rg-to-coda scattering, which can indicate an unusually shallow source.

For surface waves we have a new high-resolution regional Rayleigh-Wave tomography for the Yellow Sea and Korean Peninsula Region, based on measuring thousands of seismograms. We also continue to make new measurements for our regional Rayleigh and Love wave group velocity tomography models of Western Eurasia and North Africa. These tomography models provide high-resolution maps of group velocity from 10- to 100-s period. The maps also provide estimates of the expected phase spectra of new events that can be used in phase-match filters to compress the expected signals and improve the signal-to-noise ratio on surface wave magnitude (Ms) estimates. Phase match filters in combination with regional Ms formulas can significantly lower the threshold at which Ms can be measured, extending the Ms-mb discriminant. We have measured Ms in western Eurasia for thousands of events at tens of stations, with and without phase match filtering, and found a marked improvement in discrimination. Here we start to quantify the improvement to both discrimination performance and the Ms threshold reduction. The group velocity models also provide constraints on velocity structure, particularly in low seismicity regions. For example we are working with Dr. Bob Herrmann and Dr. Charles Ammon to combine tomography derived group velocity curves with station based receiver functions in joint inversions to estimate structure.

OBJECTIVE

Monitoring the world for potential nuclear explosions requires characterizing seismic events and discriminating between natural and man-made seismic events, such as earthquakes, mining activities, and nuclear weapons testing. We continue developing, testing, and refining size-, distance-, and location-based regional seismic amplitude corrections to facilitate the comparison of all events that are recorded at a particular seismic station. These corrections, calibrated for each station, reduce amplitude measurement scatter and improve discrimination performance. We test the methods on well-known (ground-truth) datasets in the U.S. and then apply them to the uncalibrated stations in Eurasia, Africa, and other regions to improve underground nuclear test monitoring capability.

RESEARCH ACCOMPLISHED

As part of the overall National Nuclear Security Administration Ground-based Nuclear Explosion Monitoring (GNEM) Research and Engineering (R&E) program, we continue to pursue a comprehensive research effort to improve our capabilities to seismically characterize and discriminate underground nuclear tests from other natural and man-made sources of seismicity. To reduce the monitoring magnitude threshold, we make use of regional body- and surface-wave data to calibrate each seismic station. Our goals are to reduce the variance and improve the separation between earthquakes and explosion populations by accounting for the effects of propagation and differential source size.

Body Wave Corrections

Effective earthquake-explosion discrimination has been demonstrated in a broad variety of studies using ratios of regional amplitudes in high-frequency (primarily 1- to 20-Hz) bands (e.g., Walter et al., 1995, Taylor, 1996, Rodgers and Walter, 2002, Taylor et al., 2002 and many others). When similar-sized earthquakes and explosions are nearly collocated, we can understand the observed seismic contrasts, such as the relative P-to-S wave excitation, in terms of depth, material property, focal mechanism, and source time function differences. For example in Figure 1 the top two Nevada Test Site (NTS) traces compare an earthquake and explosion of similar size and location and recorded at a common station. The traces have been high-frequency band passed at 6–8 Hz and show the characteristic discrimination difference, where the explosion has larger P wave (Pn, Pg) amplitudes relative to the S waves (Lg) when compared to the earthquake. However the third trace in Figure 1 shows another earthquake, a Hector Mine aftershock, located about 200 km farther away from the station, and it is clear that the P/S values look much more similar to those of the explosion. In reality the source P and S amplitudes for these earthquakes are nearly identical, but the farther distance the Hector Mine earthquake seismic waves have to travel to the station changes the P/S values, since the attenuation for Lg is stronger than for Pn. Clearly, if we want to discriminate between earthquakes and explosions using regional body-wave ratios, we need to account for such effects.

The availability of reference events, particularly nuclear tests, to compare to a new event in question is highly nonuniform and limited. Therefore, in many monitoring cases, we are comparing events that are not collocated, not the same size, and may have been recorded at different stations. In order to make sure any observed differences between a new event in question and the reference events (or models) are not a result of differences in path or magnitude, we must correct for these effects. In addition in order to optimally combine several different measurements to improve discrimination, we need to remove means and trends from our data. For the past several years, we have been working with our colleagues at Los Alamos National Laboratory (LANL) on the best ways to model and remove magnitude and distance trends from regional amplitudes. Last year we completed a description of the MDAC2* (a revised Magnitude and Distance Amplitude Correction) procedure that involved estimating and removing a simple theoretical earthquake spectrum from the data to remove any magnitude and distance trends in the regional phase amplitudes and any discriminants formed from those amplitudes (Walter and Taylor, 2002).

The MDAC2 model uses a more generalized version of the Brune (1970) earthquake source spectrum that allows nonconstant stress drop scaling and differential P/S corner frequency effects. We require the different phases for the same event recorded at the same station to have the same moment and apparent stress (or stress drop) values, and

* Subsequent references to calculations by MDAC in this paper were performed with MDAC2.

other source parameters, such as corner frequencies, to be related to each other. While such models of source spectra are certainly oversimplified, they have proven track records of providing good first-order fits to real earthquakes. In addition they also provide simple theoretical models to use in aseismic areas.

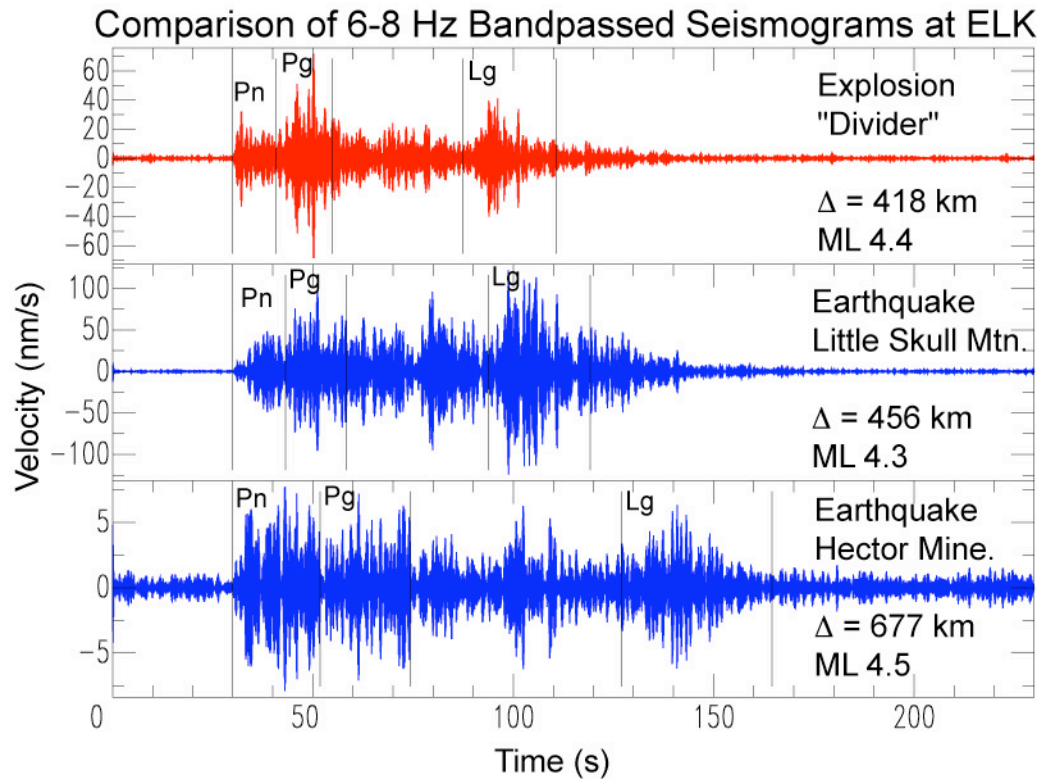


Figure 1. High-frequency (6–8 Hz band pass) seismograms of an explosion (top red) and two earthquakes (middle and bottom, blue) with similar magnitudes at auxiliary station ELK. The top two traces, both from NTS, show relative P-to-S wave amplitude differences that allow discrimination between the two source types. The bottom trace earthquake is located farther away and differential attenuation makes its P/Lg values look more like the explosion.

The details of the MDAC2 formulation are given in Walter and Taylor (2002). The predicted spectrum is a convolution of the generalized source term, geometrical spreading, site, and apparent attenuation terms. We can write the log of the MDAC2 predicted spectrum as (Walter and Taylor, 2002)

$$\log P(f, R) = \log(S_o) + \log \left[1 + \frac{\Delta^2}{c^2} \right] + \log G(R) + \text{Site}(f) + \frac{\Delta R}{Q_c} f^{(1/\Delta)} \log(e) \quad (1)$$

for a regional phase with velocity c . Here S_o is the source low-frequency spectral level and Δ/c is the source corner frequency. These terms are set by the input moment (we use the stable coda measures, see Mayeda et al, this volume), the apparent stress scaling, and material property terms. Apparent stress, geometrical spreading ($G(R)$), site effect, and attenuation (Q_c, Δ) terms are typically solved for using a grid search technique that simultaneously minimizes the spectral fit residual and residual magnitude and distance trends. In this way *a priori* information such as previous studies on geometrical spreading or Q-tomography results can be easily incorporated.

In Figure 2 we show a comparison of the observed regional phase spectra (Pn, Pg, and Lg) for some regional earthquakes recorded at station ELK with the model spectra. The calibrated MDAC Q parameters for this path are also given in this figure. For this figure we used an apparent stress scaling of $\Delta \sim M^{0.1}$, which is less than the scaling exponent of 1/4 that we found previously in the Western U.S. (Mayeda and Walter, 1996), but more than the constant stress drop value of zero. In general we find that including some apparent stress scaling improves the

regional spectral fits. The issue of whether earthquake apparent stress really increases with moment and the implications for earthquake physics remains controversial (e.g., Ide and Beroza, 2001). In a separate project, under Lawrence Livermore National Laboratory (LLNL) Laboratory Directed Research and Development (LDRD) funding, we are directly investigating apparent stress scaling using MDAC and regional coda envelope techniques. We expect those results to help the MDAC fitting process for stations in regions with low seismicity.

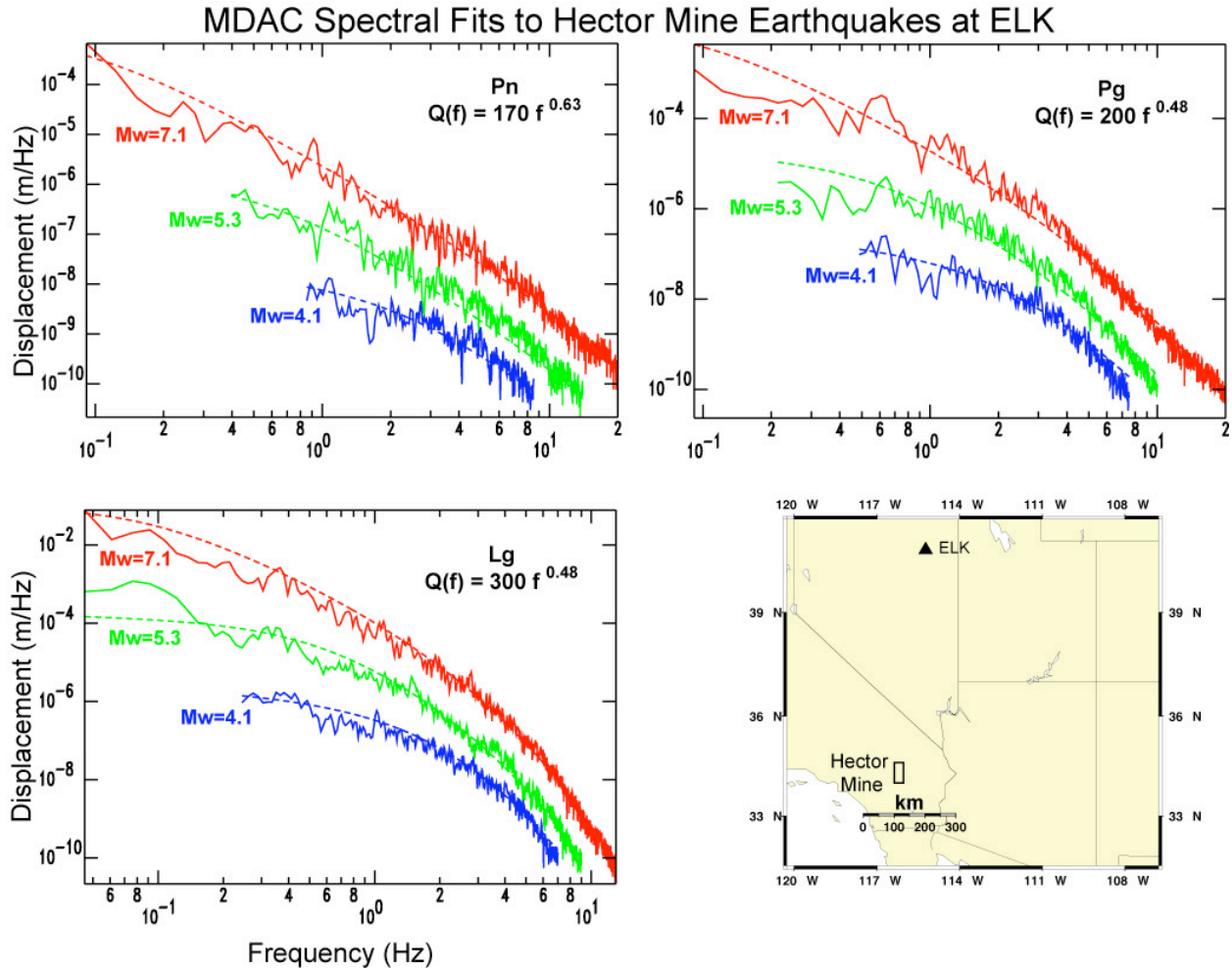


Figure 2. Comparison of the observed (solid) and MDAC2 model (dashed) spectra for the 1999 Hector Mine mainshock and two aftershocks recorded at ELK. Location map at bottom right.

For regional discrimination we can subtract these model spectra to essentially normalize the observations for effects of source, 1-D path and site. However 3-D path effects remain in the residuals. We can further reduce the MDAC2 residual amplitude variance by using the Bayesian kriging method of Schultz et al (1998) on the results. For each phase and frequency band we create kriged residual surfaces. These surfaces can then be used to create any discriminant measurement of choice. For example we can make phase, spectral, and cross-spectral ratio measurements between any phase and frequency combination. In practice it is found that the best discriminant performance comes from combining several different ratio measurements (e.g., Taylor, 1996). The MDAC (and MDAC+kriged) residuals are zero mean and roughly normally distributed, enhancing our ability to create optimized multivariate discriminant combinations using Linear Discriminant Analysis (LDA) or other techniques.

As an example of the power of combining measurements, we show in Figure 3 multivariate results (Sicherman et al., unpublished data) for some ratios at station MNV based on our earlier NTS study (Walter et al, 1995). The metric of performance we use is the equiprobable point, which provides a measure of the overlap of the earthquake and explosion populations. It is the point on an error rate receiver-operator tradeoff curve (ROC) where the error

rates are equal. For example, an equiprobable measure of 0.1 implies that 10% of the earthquakes are misclassified as explosions. In practice one might choose a decision line with unequal error rates, such as by picking a low probability of misclassifying an explosion. The equiprobable point provides a single numerical measure of performance that is much more intuitive than other measures such as Mahalanobis distance, though it can be related to that measure. From this plot we can see that multivariate combinations of measures can provide improvement over the best single measure. Equally important we can see that combining two mediocre measures (6–8 Hz Pg/Lg and 1–2/6-8 Hz Lg Coda) results in a very good discriminant. This result is important because the best single discriminant may not always be available because of phase detectability. In practice one needs to look at phase and frequency combinations with good expected signal-to-noise for the monitored region, and use those to form optimal multivariate discriminants.

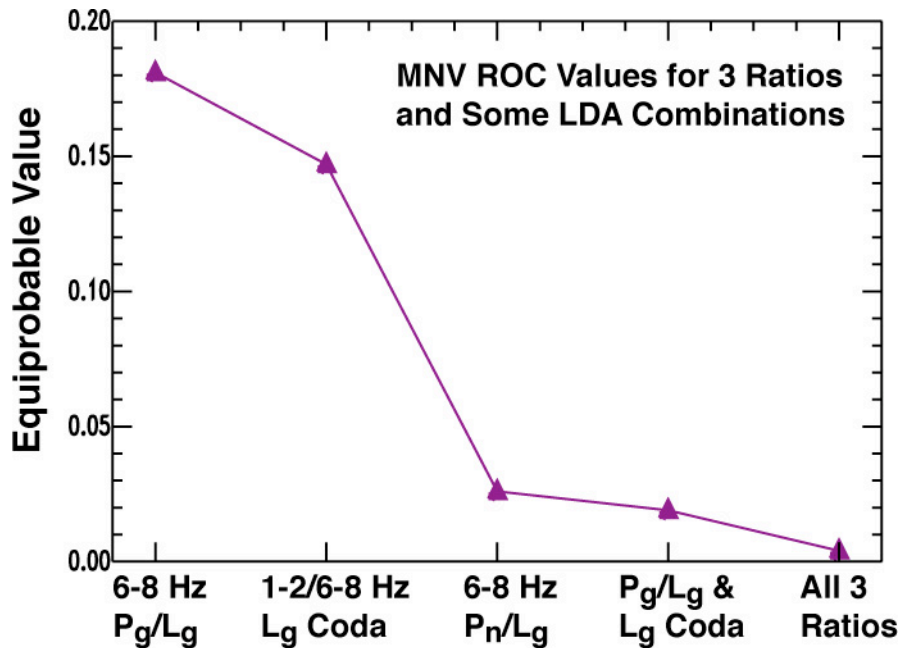


Figure 3. Discriminant performance at MNV for three individual ratio measures and two optimal LDA combinations based on data from Walter et al. (1995).

This issue of phase detectability is often overlooked in regional discrimination studies, but it is of critical importance. A great discriminant measure based on training data that is not detectable for all the magnitude, phase, and frequencies is of limited use. In order to truly evaluate discriminant performance, we need to map out ahead of time the expected signal-to-noise values as a function of magnitude, phase, and frequency. Fortunately the calibrated MDAC curves provide a straightforward means to do this mapping for earthquakes. In Figure 4 we show the expected 6–8 Hz RMS (root mean square) displacement amplitudes for an Mw 4.0 earthquake recorded at station ELK for the calibrated MDAC parameters discussed in Figure 2. For events within approximately 800 km of ELK, the Lg phase has the largest amplitude and beyond this distance, the P phases (Pn and Pg) dominate. We also put an average noise level for ELK on the plot, making it immediately apparent that there will be detectability issues for Lg beyond about 1,000 km and for Pn and Pg beyond about 1,200 km at 6–8 Hz for a Mw 4.0 and smaller earthquakes. If we were interested in using ELK to discriminate such small magnitude events at distances larger than about 1,000 km, then we need to choose different discriminant measures than those shown in Figure 3. In practice the picture is complicated further by 2-D effects, which we have ignored so far. In data rich areas we can use the kriging results to modify the curves by region; in data poor areas we can use Q tomography models. For optimal regional discrimination we calibrate the MDAC parameters for each station and use them both to determine the detectable phases we have to work with and the normalized measures to combine with multivariate techniques.

Finally in Figure 4 we can also easily ratio any of predicted amplitude curves to show the expected behavior of particular discriminant ratios as functions of distance, magnitude, or frequency. Here we show the P/Lg ratios with their strong distance dependence. From the figure we expect about a factor of 2 difference in the P/Lg ratios for the events at 450 km versus 680 km, consistent with what we saw in the data in Figure 1.

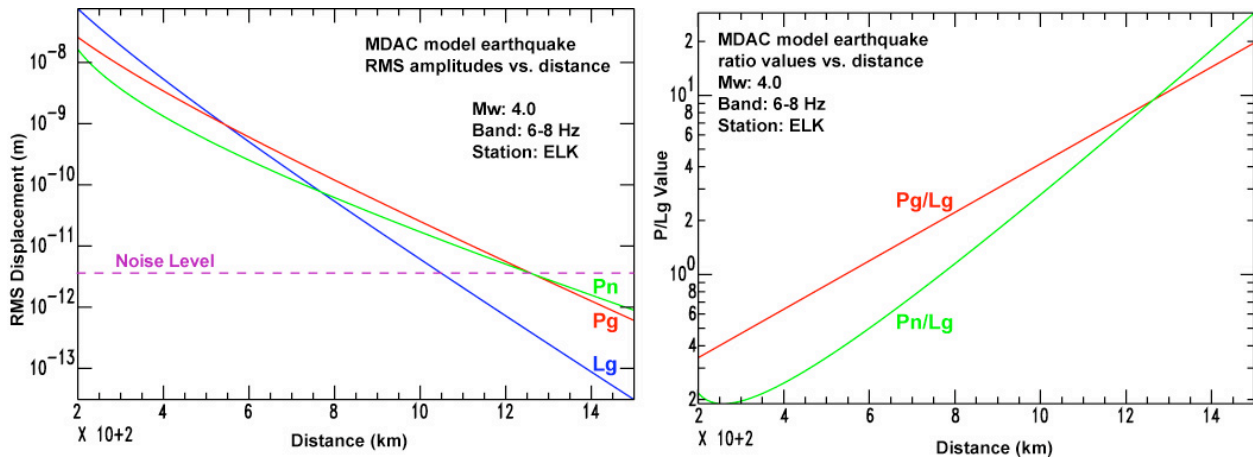


Figure 4. Predicted MDAC earthquake regional phase values as functions of distance from ELK. The calculations are done for an Mw 4.0 event at 6-8 Hz using attenuation parameters from Figure 2. Left-hand side shows RMS amplitude versus distance; right-hand side shows P/Lg ratio values versus distance.

Surface Wave Corrections

The teleseismic magnitude ratio $M_S:m_b$ is one of the best-understood and most effective discriminants known (e.g., Stevens and Day, 1985). Several studies have also shown that it appears to be effective down to as small magnitudes as can be measured regionally (e.g., Denny et al., 1987). The problem is that the 20-second surface-wave amplitude on which M_S is based can be below the noise even at regional distances. We are researching several ways to allow M_S measurements on smaller magnitude events to be made and used to improve discrimination. One way is to allow regional M_S measurements at periods between 10 and 20 s where the regional Airy phase produces the largest amplitudes (e.g., Denny et al., 1987). Additionally we can improve signal-to-noise by making use of phase-match filters (e.g., Herrin and Goforth, 1977). This use of phase-match filters is particularly attractive because in addition to reducing the noise level in the signal, it can provide an accurate maximum M_S estimate even on a very noisy trace. For small explosions that have reduced M_S excitation to start with and may not have observable surface waves, this method can still provide some discrimination power relative to earthquakes of the same m_b that do have measurable M_S .

For the past several years we have been making systematic measurements of Rayleigh and Love wave group velocities in Western Eurasia and North Africa (WENA) with the goal of creating high-resolution tomography models (Pasyanos et al., 2001). We follow the guidelines for measurements laid out in the 1998 surface-wave workshop (Walter and Ritzwoller, 1998), and we have exchanged group velocity curves with other groups. We have incorporated more than 3,000 path measurements from the University of Colorado (Ritzwoller, written communication) and SAIC/Maxwell (Stevens, written communication). We have used the software code PGSWMFA developed by Dr. Charles Ammon to measure thousands of seismograms from the LLNL Seismic Research database (see O'Boyle et al., this volume) over the past several years. The tomography maps that we have created are formed from both our own regional measurements and the broader measurements provided by those two groups. We have also benefited from IRIS (Incorporated Research Institutions in Seismology) PASSCAL (Program for the Array Seismic Studies of the Continental Lithosphere) deployments in Africa and Arabia to supplement the (IMS) International Monitoring System, IRIS Global Seismic Network (GSN) and other open stations.

Overall, in the WENA region we have examined more than 25,000 seismograms and made more than 15,500 Rayleigh wave measurements and 10,000 Love wave measurements at periods from 8–150 seconds. These measurements are an increase of about 5,000 Rayleigh and Love measures each over our tomography models from last year. These numbers apply to the middle period range and the number of good measurements decreases at the

shorter and longer periods. In Figure 5 we show the WENA tomography results for Rayleigh waves at one period, 20 seconds. At this period crustal thickness differences between oceanic and continental crust are clear. Deep sedimentary basins (e.g., Caspian depression, Mesopotamian foredeep) also stand out as very slow areas. For reference we also show the path map with earthquake and station locations. Overall the coverage is quite good, although the lack of stations and seismicity in Western Africa and Northern Russia remains a challenge.

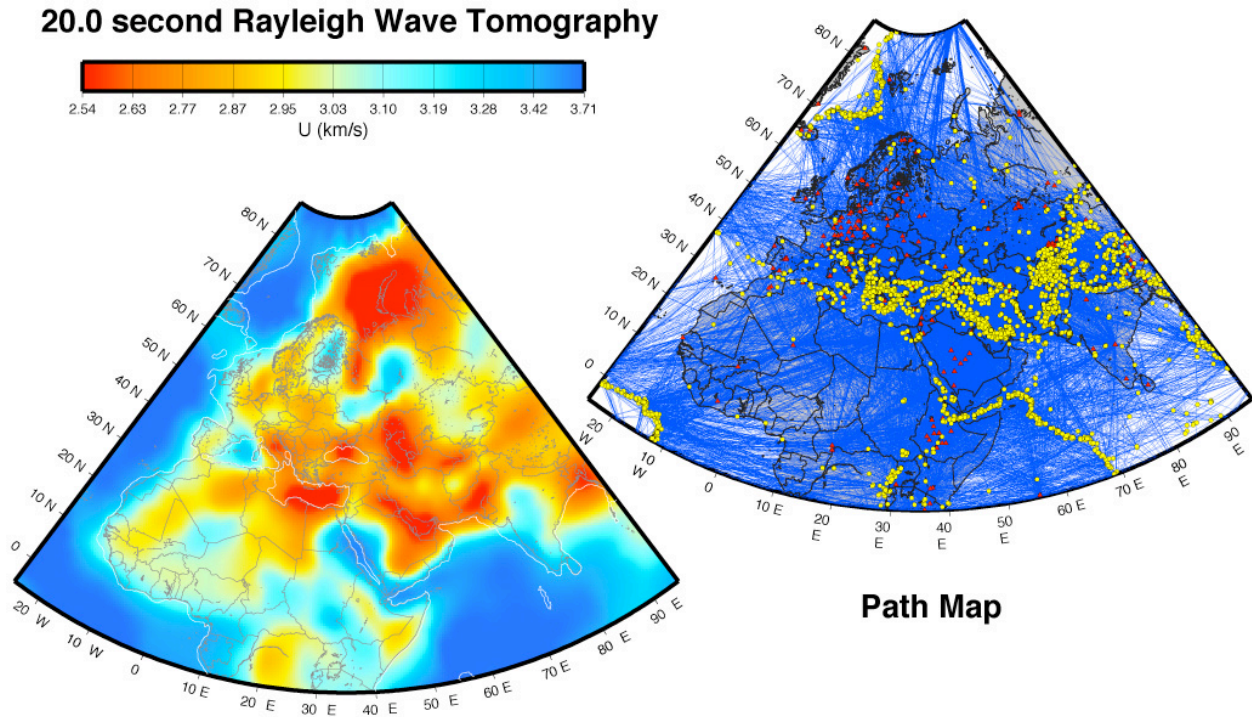


Figure 5. Rayleigh wave group velocity tomography and path map at 20-second period for the WENA region.

Last year we demonstrated the improvement provided by phase-match filtering on M_s - m_b in Western Eurasia (Walter et al. 2002). For that test we measured M_s using the formula of Rezapour and Pearce (1998). The maximum likelihood M_s was measured both by traditional band pass filtering and after phase-match filtering using the high-resolution tomography model. We tried a variety of tests in which we varied the signal-to-noise ratio (SNR) or number of stations. We found that in almost all cases phase-match filtering improves the M_s - m_b discrimination by approximately a factor of two. We also estimate that phase match filtering is able to lower the M_s detection measurement threshold by roughly 0.3 magnitude units or a factor of two. Both these effects, improved discrimination performance and lower M_s measurement thresholds, indicate that using phase-match filtering for the M_s measurement can significantly improve discrimination performance.

Recently we have started making surface-wave dispersion measurements in the Yellow Sea—Korean Peninsula (YSKP) area in order to make a high-resolution tomography model for that region as well. Again we have greatly benefited from IRIS PASSCAL deployments in China and North Korea, as well as from the South Korean regional seismic network data (B. Herrmann, written communication). So far we have examined about 6,500 seismograms and made 5,000 Rayleigh wave measurements. In Figure 6 we show the group-velocity tomography results and the path map for 20-second period Rayleigh waves. We have used a new variable-grid smoothing algorithm in this result. As in the WENA tomography, the oceanic regions of the Sea of Japan and the Pacific show up as relatively fast velocities. Again deep sedimentary basis such as the Bohai in the northwest part of the Yellow Sea are slow. However path coverage remains poor outside of the Yellow Sea, Korean Peninsula and Sea of Japan. As we continue to make measurements, we expect to be able to combine these two separate tomographies into a single

large-scale tomography of Eurasia and Africa that will provide very good coverage of nearly the entire continental region.

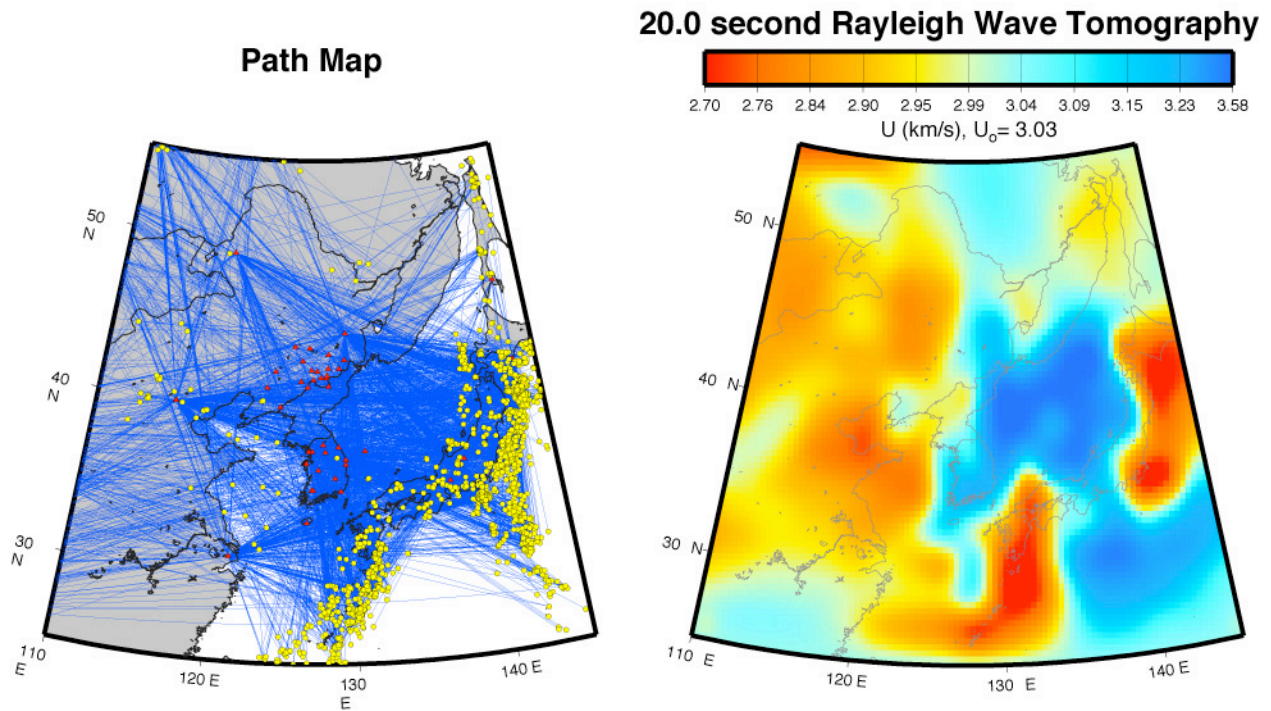


Figure 6. Rayleigh wave path map and group velocity tomography map at 20 seconds period for the YSKP region.

Finally the surface wave tomographies shown in Figures 5 and 6 provide information about the underlying velocity structure that may prove useful for location calibration, particularly in aseismic regions. We have used the WENA tomography to test an LLNL *a priori* model (see Pasyanos et al., this volume). We are currently using the surface wave tomography model in conjunction with receiver functions to estimate velocity structure in Western Eurasia (see Ammon et al., this volume) and the YSKP region with Dr. Bob Herrmann.

CONCLUSIONS AND RECOMMENDATIONS

Regional discrimination algorithms require calibration at each seismic station to be used for nuclear explosion monitoring. We have developed a revised Magnitude and Distance Amplitude Correction procedure to remove source size and path effects from regional body-wave phases. This procedure allows the comparison of any new regional events recorded at a calibrated station with all available reference data and models. It also facilitates the combination of individual measures to form multivariate discriminants that can have significantly better performance. We have also developed surface-wave group velocity maps and correction surfaces for phase-match filtering to improve Ms-mb discrimination and lower its effective threshold. Calibrating seismic stations to monitor for nuclear testing is a challenging task that will require processing large amounts of data, and collaboration with government, academic and industry researchers and incorporation of the extensive R&D results both within and outside of NNSA.

ACKNOWLEDGEMENTS

We thank Steve Taylor at LANL for many discussions on the topics of MDAC and regional discrimination. We thank Mike Ritzwoller and Jeff Stevens for generously sharing their group velocity measures. We thank Maggie

Benoit for making many new East Africa dispersion measurements this summer. We thank the many scientists for their efforts in providing open station data from PASSCAL, GSN and IMS, and other networks.

REFERENCES

- Brune, J. N. (1970). Tectonic stress and seismic shear waves from earthquakes, *J. Geophys. Res.* **75**, 4997-5009.
- Denny, M. D., S. R. Taylor, and E. S. Vergino (1987). Investigation of mb and Ms formulas for the western United States and their impact on the Ms/mb discriminant, *Bull. Seism. Soc. Am.*, **77**, 987-995.
- Herrin, E. and T. Goforth (1977). Phase-matched filters: Applications to the study of Rayleigh waves, *Bull. Seism. Soc. Amer.*, **67**, 1259-1275.
- Ide, S. and G. C. Beroza (2001). Does apparent stress vary with earthquake size?, *Geophys. Res. Lett.* **28**, 3349-3352.
- Mayeda, K. M. and W. R. Walter, (1996). Moment, energy, stress drop and source spectra of Western U.S. earthquakes from regional coda envelopes, *J. Geophys. Res.*, **101**, 11,195-11,208.
- Pasyanos, M. E., W. R. Walter and S. E. Hazler (2001). A surface wave dispersion study of the Middle East and North Africa for monitoring the comprehensive nuclear-test-ban treaty, *Pure Appl. Geophys.*, **158**, 1145-1474.
- Rezapour, M. and R. G. Pearce (1998). Bias in surface wave magnitude Ms due to inadequate distance corrections, *Bull. Seism. Soc. Am.*, **88**, 43-61.
- Rodgers, A. J. and W. R. Walter, (2002). Seismic Discrimination of the May 11, 1998 Indian Nuclear Test with Short-Period Regional Data From Station NIL (Nilore, Pakistan), *Pure Appl. Geophys.* **159**, 679-700.
- Schultz, C, S. Myers, J. Hipp, and C. Young (1998). Nonstationary Bayesian kriging: a predictive technique to generate corrections for detection, location and discrimination, *Bull. Seism. Soc. Am.*, **88** 1275-1288.
- Stevens, J. L. and S. M. Day (1985). The physical basis of mb:Ms and variable frequency magnitude methods for earthquakes and explosion discrimination, *J. Geophys. Res.*, **90**, 3009-3020.
- Taylor, S., (1996). Analysis of high-frequency Pg/Lg ratios from NTS explosions and Western U.S. earthquakes, *Bull. Seism. Soc. Am.*, **86**, 1042-1053.
- Taylor, S., A. Velasco, H. Hartse, W. S. Philips, W. R. Walter, and A. Rodgers, (2002). Amplitude corrections for regional discrimination, *Pure. App. Geophys.* **159**, 623-650.
- Walter, W. R., K. Mayeda, and H. J. Patton, (1995). Phase and spectral ratio discrimination between NTS earthquakes and explosions Part I: Empirical observations, *Bull. Seism. Soc. Am.*, **85**., 1050-1067.
- Walter, W. R. and M. Ritzwoller, (1998). Summary report of the workshop on the U.S. use of surface waves for monitoring the CTBT, Lawrence Livermore National Laboratory *UCRL-ID-131835*, 16 pp.
- Walter, W. R. and S. R. Taylor (2002), A revised Magnitude and Distance Amplitude Correction (MDAC2) procedure for regional seismic discriminants, Lawrence Livermore National Laboratory *UCRL-ID-146882*.
- Walter, W. A. Rodgers, M. Pasyanos, K. Mayeda, and A. Sichermann, (2002). "Identification in western Eurasia: Regional body-wave corrections and surface-wave tomography models to improve discrimination," in "Proceedings of the 24th Seismic Research Review: Nuclear Explosion Monitoring: Innovation and Integration," Los Alamos National Laboratory, *LA-UR-02-5048*.